7th EUROMECH Solid Mechanics Conference
J. Ambrosio et.al. (eds.)
Lisbon, Portugal, 7–11 September 2009

EXPERIMENTAL OBSERVATION OF SINGLE MODE PANEL FLUTTER IN SUPERSONIC GAS FLOW

Vasily V. Vedeneev[1], Sergey V. Guvernyuk[1], and Mikhail E. Kolotnikov[2]

[1]Lomonosov Moscow State University
1, Leninskie Gory, Moscow, Russia
e-mail: vasily@vedeneev.ru, guv@mail.ru

[2] MMBPP "Salut"
16 Budionny Av., Moscow, Russia
e-mail: kolotnikov@salut.ru

Keywords: Flutter, Panel Flutter, Plate Flutter, Vibrations, Aeroelasticity.

Abstract. *Single mode flutter is a type of panel flutter, which cannot be analyzed theoretically using conventional piston theory, and for this reason it is studied very little. No previous experiments, where this type of panel flutter was detected, were conducted. In this paper a plate, designed such that it cannot experience "classical" coupled-type flutter, but can experience single mode flutter, is tested. Analysis of the tested data clearly indicates the occurrence of single mode panel flutter.*

1 INTRODUCTION

Panel flutter is an aeroelastic phenomenon that is known to cause fatigue damage of flight vehicles. Let us imagine a skin panel of a flight vehicle in a supersonic gas flow, for example, in Figure 1 a wing skin panel is shown. If the flow speed is relatively low, then the static state of the panel is stable. Once the critical speed (or the critical Mach number, M_{cr}) is exceeded, the static state of the panel becomes unstable, and the panel vibrates. This vibration occurs due to energy transfer from the gas flow to the panel. The amplitude of this vibration can be large and result in fatigue damage of the panel and the structures attached to the panel.

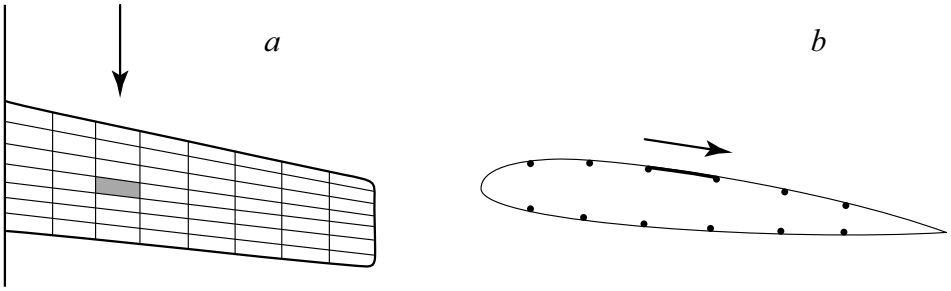

Figure 1: Skin panel is a typical structure subjected to panel flutter.

This problem of panel flutter was first observed during the 1940s and has since had a very rich history. Theoretical solution of the problem consists of an eigenvalue solution of coupled panel-flow equation. Let us assume that the plate deflection is harmonic: $w(x,t) = W(x)e^{-i\omega t}$ (for simplicity we demonstrate up-to-date theory on 2D problem), the equation of the plate motion takes the form

$$D\frac{\partial^4 W}{\partial x^4} - \omega^2 W + p\{W,\omega\} = 0 \tag{1}$$

where D is the plate stiffness, and $p\{W,\omega\}$ is the pressure acting on the oscillating plate. The theory of potential gas flow gives expression [1]

$$\begin{aligned} p\{W,\omega\} = \frac{\mu M}{\sqrt{M^2-1}}\left(-i\omega W(x) + M\frac{\partial W(x)}{\partial x}\right) + \\ + \frac{\mu\omega}{(M^2-1)^{2/3}}\int_0^x \left(-i\omega W(\xi) + M\frac{\partial W(\xi)}{\partial \xi}\right)\cdot \\ \cdot \exp\left(\frac{iM\omega(x-\xi)}{M^2-1}\right)\left(iJ_0\left(\frac{-\omega(x-\xi)}{M^2-1}\right) + MJ_1\left(\frac{-\omega(x-\xi)}{M^2-1}\right)\right)d\xi \end{aligned} \tag{2}$$

Substitution of this expression into equation (1) yields the complex integro-differential equation. Solving this equation is difficult, however, in the 1950s a relatively simple theory, known as the piston theory, was developed to approximate the gas pressure. This theory, shown in equation (3), neglects the integral terms from equation (2), therefore it is valid only at high Mach numbers and low frequencies:

$$p\{W,\omega\} = \frac{\mu M}{\sqrt{M^2-1}}\left(-i\omega W(x) + M\frac{\partial W(x)}{\partial x}\right) \tag{3}$$

This partial-differential equation (1), (3) can be easily solved numerically and studied analytically. Piston theory has been the primary analysis method used by aeroelasticians. An enormous number of panel flutter publications have used the more simplistic piston theory but only a few authors have published work regarding the exact theory of potential flow [2, 3, 4, 5, 6, 7]. Up to our days, most complications in studies of panel flutter are related with structures studied, while air pressure is calculated using the piston theory (3).

Though piston theory is a simple approach used to predict flutter it also has a serious problem. Two types of panel flutter are known [8]. First, the coupled-type flutter arising due to the interaction of two eigenmodes. This type has been fully studied through the piston theory, and excellent correlation with experiments at $M > 1.7$ has been observed. The second flutter type is single mode flutter also referred as "single-degree-of-freedom" or "high-frequency" flutter. This flutter type can only be analyzed through exact aerodynamic theory of potential flow or more complex theories. Until recently, only in a few publications discussed single mode flutter was mentioned [2, 4, 8], where it was obtained through direct numerical simulations, however, the energy transfer mechanism was not studied. This flutter type has not been thoroughly investigated, some have even suggested that it may not appear in reality. However, over the past few years single mode flutter was studied in detail [9, 10, 11, 12], and a simple physical explanation of instability has been derived. Previously, there have been no documented reports where this flutter has been observed experimentally. This paper explains the analysis method and experiments conducted to confirm the existence of single mode flutter.

Tests focusing on single mode flutter have been conducted at the Institute of Mechanics of Moscow State University. These experiments used a clamped plate, which have been designed such that coupled-type flutter can not occur during wind tunnel testing. At the same time, single mode flutter should occur. Gages used during the experiment allow for monitoring of the plate vibrations and the vibration source. The results clearly show that the plate vibrations correspond to the existence of single mode flutter.

2 DESCRIPTION OF THE EXPERIMENT

The experiment setup is shown below in Figure 2. The tested specimen is a flat plate made from steel and welded to a rigid frame. The frame has been fixed to the wind tunnel wall. The plate size was $300 \times 540 \times 1$ mm. A cavity under the plate allows for gas flow to bypass under the plate, which equalizes the pressure between both sides of the plate.

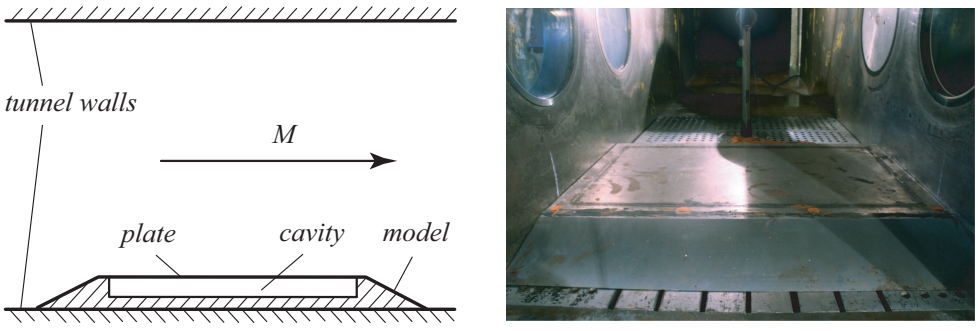

Figure 2: Sketch of the test (left). Picture of the model installed into the tunnel (right).

To monitor plate vibrations, 12 strain gages were installed on the "cavity" side of the plate. The gage signals were amplified and operated in the range of 20 – 10000 Hz. A vibro gage

AP2037 was installed on outside tunnel wall to monitor wind tunnel vibrations. This gage was used with transformator AS02. Flow pressure pulsations were monitored by means of the Honeywell pressure gage, 186PC15DT. Figure 3 depicts the setup configuration by which measurements have been taken during the experiment.

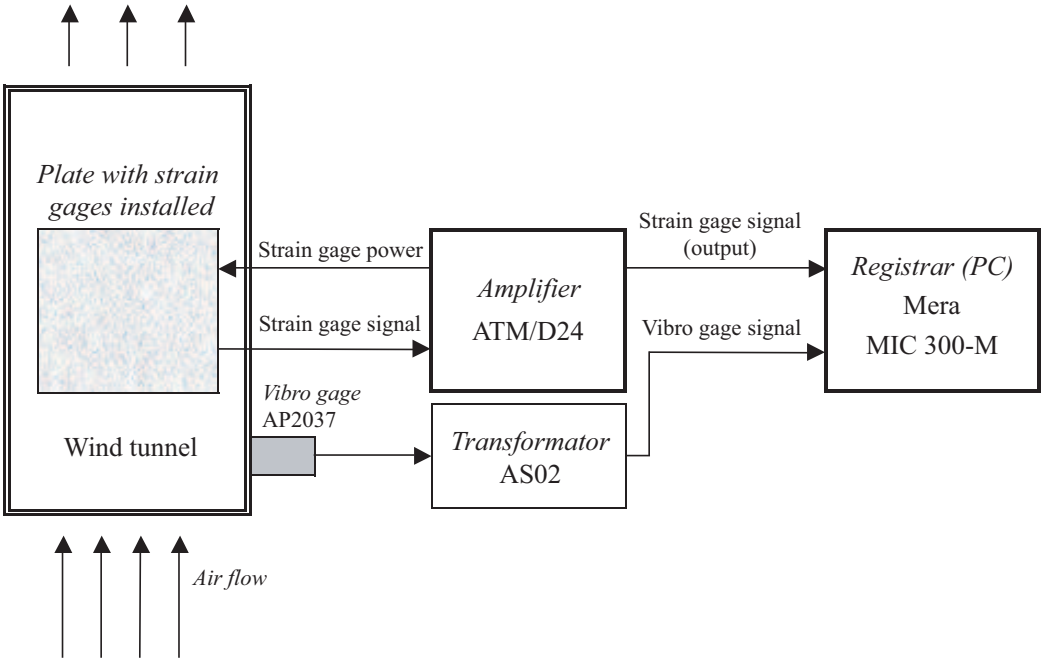

Figure 3: Scheme of the test measurements (pressure gage is not shown).

Generally, five sources of high-amplitude plate oscillations could occur during the test:

1. Resonance excited by vibrations of the wind tunnel
2. Resonance excited by pulsations of the flow pressure
3. Responce to noise excitation
4. Coupled-type panel flutter
5. Single mode panel flutter

Identifying the actual plate vibrations type is possible through spectral analysis of the plate strain gages, tunnel vibro gage and the pressure gage spectrum data. Let us describe signs, which allow to exclude or confirm types of the plate oscillations.

Resonance excited by vibrations of the wind tunnel can be easily recognised by comparing the spectrums of the plate strain gages and the tunnel vibro gage. If high-amplitude peaks exist in these spectrums with the same frequencies, then the wind tunnel has caused the plate vibrations. On the contrary, if the plate oscillates at a different frequency than that of the vibro gage, then the first type of vibrations is excluded.

In the same way, resonance excited by pulsations of the flow pressure can be easily detected by comparing spectrums of the plate strain gages and the flow pressure gage.

Noise excitation of the plate vibrations can be detected comparing vibration amplitudes at several regimes of the wind tunnel (for example, at several Mach numbers). If while changing

Mach number, M, both the amplitudes of noise vibrations of the tunnel and noise pulsations of the flow pressure increase, while amplitude of the plate vibrations decreases or increases at a much faster rate than the noise amplitude (or vice versa), then these vibrations cannot be caused by noise excitation.

Coupled-type flutter can be detected using its main feature: it occurs due to interaction of two eigenmodes, which can be detected by approaching and coalescence of the first and the second eigenfrequencies. Thus, if the amplitude increases sharply, while the two mentioned eigenfrequencies do not approach to each other, we exclude coupled-type flutter from the list of possible sources of vibrations.

3 THEORETICAL FLUTTER PREDICTIONS

The plate size was chosen such that coupled-type flutter would not occur. The critical Mach number for coupled-type flutter was computed by applying formula [13] obtained through the piston theory:

$$M_{cr} = \frac{D}{p\gamma L_x^3}\frac{8\pi^3}{3\sqrt{3}}\left(5+\frac{L_x^2}{L_y^2}\right)\sqrt{2+\frac{L_x^2}{L_y^2}}, \tag{4}$$

where L_x and L_y are the plate width and length (air flows along x direction), D is the plate stiffness, p is a static pressure of the flow, γ is an adiabatic constant of the air. Static pressure in the wind tunnel changes with change of actual Mach number M. Using this isentropic formula

$$p(M) = p_0\left(1+(\gamma-1)\frac{M^2}{2}\right)^{-\frac{\gamma}{\gamma-1}}$$

and parameter p_0 typical for the used wind tunnel, we obtain function $M_{cr}(M)$. Equation (4) is derived for a pinned plate, which implies M_{cr} is higher for a clamped plate. Figure 4 shows the plot $M_{cr}(M)$ for parameters of the wind tunnel used, where we can see that $M_{cr} > M$ for any M, and thus coupled-type flutter is impossible.

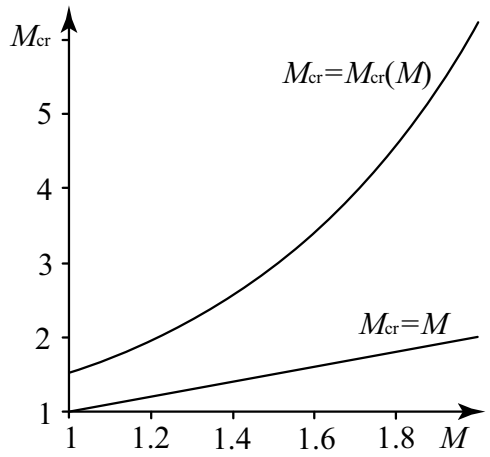

Figure 4: Plot $M_{\rm cr}(M)$ defined by (4). Additionally a line $M_{\rm cr} = M$ is shown.

On the contrary, single mode flutter should arise at the test conditions. For theoretical analysis the method [10] is used. Following that paper, for each eigenmode (m, n) (the first number in brackets is quantity of semi-waves in the mode along the flow (short) direction, the second number is the one along the long direction) there is a region of single mode flutter

$M_1(m,n) < M < M_2(m,n)$. We consider only modes fluttering at $M < 1.3$, as the tests were conducted at $M < 1.3$. Calculated values of M_1 and M_2 are shown in Table 1.

m	n	Frequency Ω (Hz)	M_1	M_2
1	1	65	1.19	1.56
2	1	167	1.17	1.48
2	2	190	1.28	1.61
3	1	321	1.20	1.48
3	2	344	1.26	1.54
4	1	526	1.25	1.49
4	2	549	1.29	1.53

Table 1: Eigenmodes which are unstable in region $M < 1.3$ and their flutter regions.

Thus, during the test in spectrum of the plate oscillations we should see some of 7 modes: (1,1), (2,1), (2,2), (3,1), (3,2), (4,1), (4,2) at corresponding frequencies. More detailed analysis shows that increments of amplification are the biggest at modes (1,1) and (2,1), in other words, these modes are most unstable.

In Table 1 we did not take into account influence of factors considered in Section 4. Below we will show that the frequency of the mode (1,1) is higher, and this mode should excite at higher M than shown in the table, while flutter region for the mode (2,1) is the same.

4 NATURAL PLATE OSCILLATIONS

In order to verify dynamic properties of the test model produced, initially a natural mode experiment was conducted. A light strike of a mallet was made, while strain gage data was recorded and analysed. Test spectrums are shown in Figure 5. From flutter point of view, the most important eigenmodes are (1,1) and (2,1). Test result is 143 Hz for the mode (1,1) and 170 Hz for the mode (2,1). Classical formula for a free clamped plate eigenfrequencies yields 65 Hz for the mode (1,1) and 167 Hz for the mode (2,1) (see Table 1). We can see that there is an excellent correlation between theory and test data for the mode (2,1), while for the mode (1,1) there is a paradoxical inconsistency.

In order to understand sources of this inconsistency, influence on eigenfrequencies of several parameters, not controllable in the test, was studied using Abaqus FE software. Several factors influencing natural oscillations, as well as plate vibrations during tests in the wind tunnel, were considered: temperature of the plate, initial out-of-plane deflection, and air pressure in the cavity. Let us consider them in series.

Temperature of the plate can be different from temperature of other parts of the test assembly. Indeed, when the wind tunnel is just launched, cold air flow cools thin plate faster then its thick frame, and temperature strains lead to increase of eigenfrequencies. With time, the frame also cools, temperature strains disappear, and eigenfrequencies decrease down to values of unstretched plate in vacuum. The plate temperature modelled is $-5\ ^o$C relative to the frame.

The plate had out-of-plane static deflection due to residual stress after welding. Unfortunately, this stress was not fully eliminated, and the plate was slightly buckled with maximum out-of-plane displacement 2 mm. In FE model residual plate deflection was modelled directly:

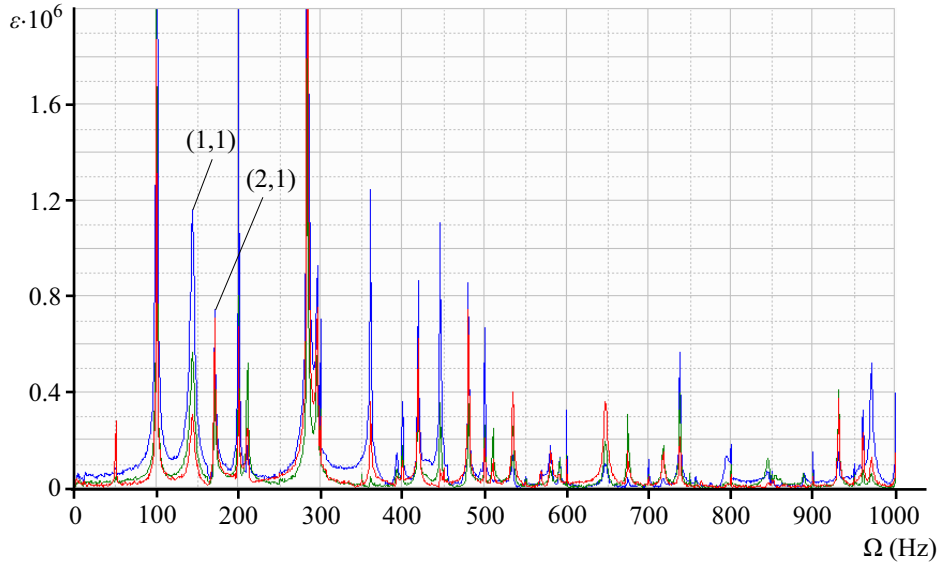

Figure 5: Spectrum of plate strain gage data. The plate is excited by slight impact of a mallet. All peaks with frequencies proportional to 50 and 100 Hz are electrical interferences and should be ignored.

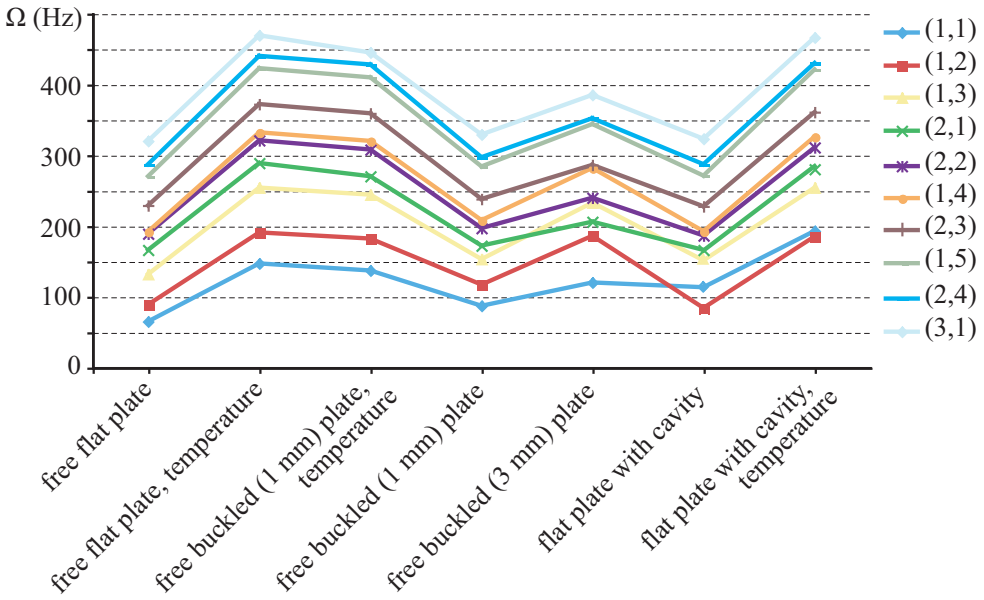

Figure 6: Influence of non-controllable factors on the plate eigenfrequencies.

plate shape in the FE model was the same as the real plate shape. Two amplitudes of buckling were considered: 1 mm and 3 mm. Both ones were modelled, because buckling amplitude could vary or eliminate at all during the test because of temperature strains.

The last considered factor, air pressure in the cavity (Figure 2) is the most interesting one. If the plate oscillates at symmetric eigenmode (for example, at mode (1,1)), then volume of the cavity, as well as air pressure, changes. Thus the cavity works as ”aerodynamic spring”. On the contrary, if the plate oscillates at antisymmetric mode (for example, (2,1)), then the cavity volume does not change, and the cavity does not affect oscillations.

Results of the modelling are shown in Figure 6. We can see that at natural oscillations out of

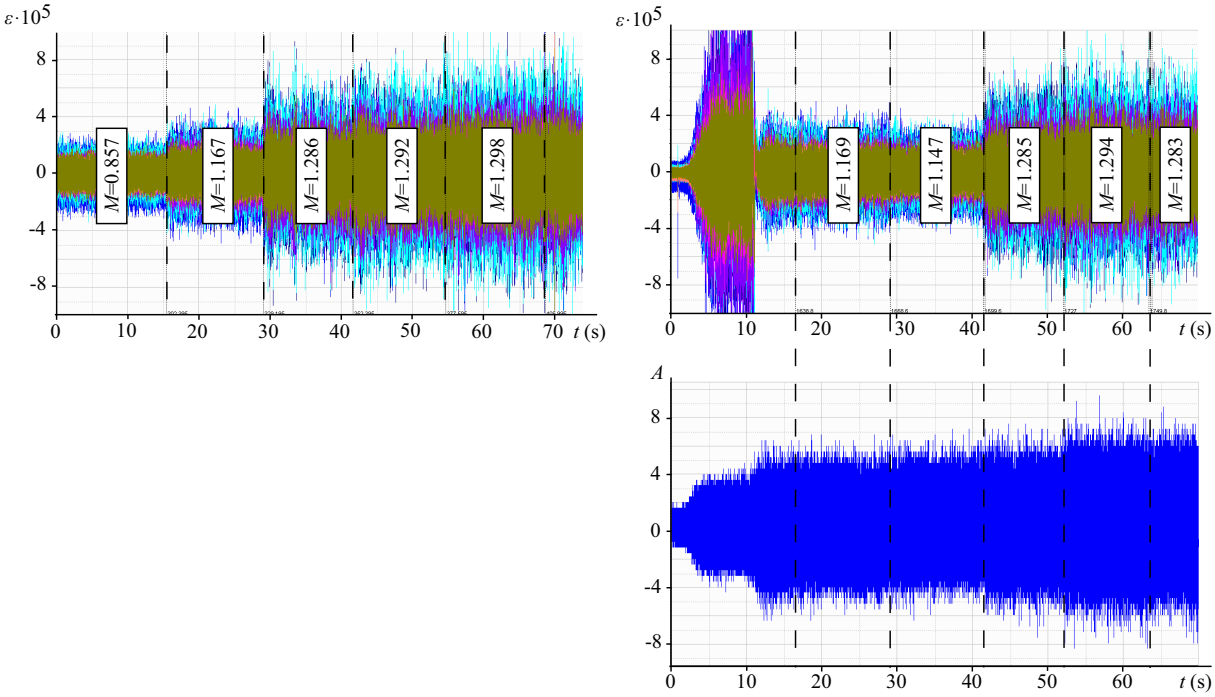

Figure 7: Amplitude of the plate (top) and the wind tunnel wall (bottom) vibrations during launch 1 (left, tunnel vibrations were not recorded) and launch 2 (right).

the wind tunnel (no temperature effect) the only factor explaining inconsistency between theory and experiment is the cavity air pressure. Exactly as physical arguments predict, it works as an "aerodynamic spring" at symmetrical oscillation modes, and does not affect antisymmetrical modes. These results also show that residual plate stess after welding does not affect natural oscillation at the mode (2,1), as the test frequency of this mode is the same as unstressed plate theory predicts.

Figure 6 also shows possible behaviour of the plate eigenfrequencies during launch of the wind tunnel, when temperature of the plate is lower then temperature of the frame. We can see that frequencies grow dramatically even at slight change of the temperature. This fact is fully confirmed by tests in the wind tunnel: frequencies just after launch were much higher then frequencies before the launch, and were decreasing with time.

5 RESULTS OF THE EXPERIMENT

The test was conducted at eleven regimes of the wind tunnel. Corresponding Mach numbers are $M = 0.857, 1.147, 1.167, 1.169, 1.285, 1.286, 1.292, 1.293, 1.294, 1.298$, these values are intentionally shown with accuracy 0.001. Of course, the pressure gage did not allow to conduct measurements with such a high accuracy. But important is the fact that ordering of the regimes by M is correct. In other words, despite Mach number values are inaccurate, from inequality $M_1' < M_2'$ (where stroke denotes inaccurately measured value) it follows ineqaulity $M_1 < M_2$ for exact values. This is the goal of usage of three digits after decimal point.

In Figure 7 shown are the plate strain amplitudes vs time for two launches of the wind tunnel. Plate strain amplitudes vs Mach number for these tests are shown in Figure 8.

We can see rapid amplitude growth in region $1.2 < M < 1.3$. Let us now analyse source of this growth.

In Figures 9, 10, 11 shown are typical spectrums of the plate strain gages, tunnel vibro gage, and static pressure gage. In Figure 9 we see that amplification of plate oscillations occurs due

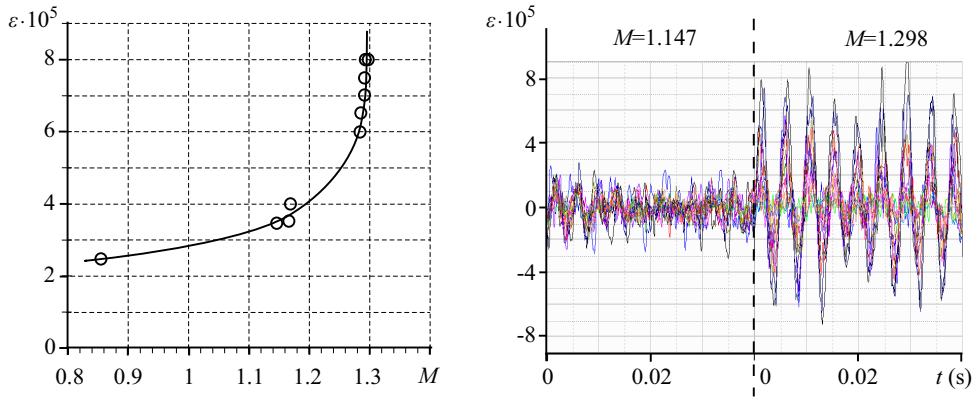

Figure 8: Left: dynamic strain amplitude vs Mach number. Test data is shown by points, the curve is an interpolation. Right: temporal strain data at $M = 1.147$ (stability) and 1.298 (flutter).

to amplification of five spectrum peaks: 170 Hz, 215 Hz, 320 Hz, 400 Hz, and 505 Hz. At the same time, flow pressure and tunnel vibration spectrums have no notable spectrum peaks at all regimes, and thus plate oscillations are not of the first two types (resonances) specified in Section 2.

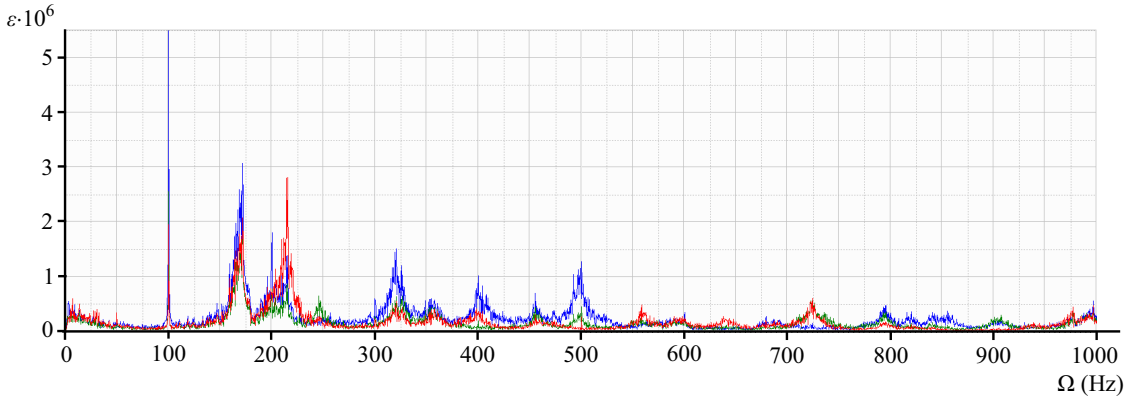

Figure 9: Spectrum of the plate vibration at regime $M = 1.298$. All peaks with frequencies proportional to 50 and 100 Hz are electrical interferences and should be ignored.

Let us now consider the third possible source of amplification of the plate vibrations, noise excitation. If the amplification occurs due to this reason, then noise amplitude (pressure pulsations or tunnel vibrations, depends on which one excites the plate) at different regimes should have the same trend as the plate amplitude. But measurements (from Figure 7, for example) show that amplitude of pressure pulsation and tunnel vibrations increase not more than 1.3 times at launch 2, while the plate amplitude increases more than 2 times. Thus, the third source of excitation of the plate vibrations, noise, is also excluded from the list of possible sources.

The forth source of amplification of the plate vibrations, coupled-type flutter, is impossible due to theoretical analysis (Figure 4). This also can be proved using test data only. Indeed, let us consider sequence of spectrums of plate vibrations at M increasing, showed in Figures 12, 13, 14, and 9. If coupled-type flutter occurs, then, following theory, frequencies of modes (1,1) and (2,1) should aprroach to each other and merge. Analysis of amplitude distribution along strain gages shows that in the spectrums the peak with frequencies 190 Hz at $M = 1.147$, 180 Hz at $M = 1.167$, 160 Hz at $M = 1.286$, and 170 Hz at $M = 1.298$, corresponds to the mode

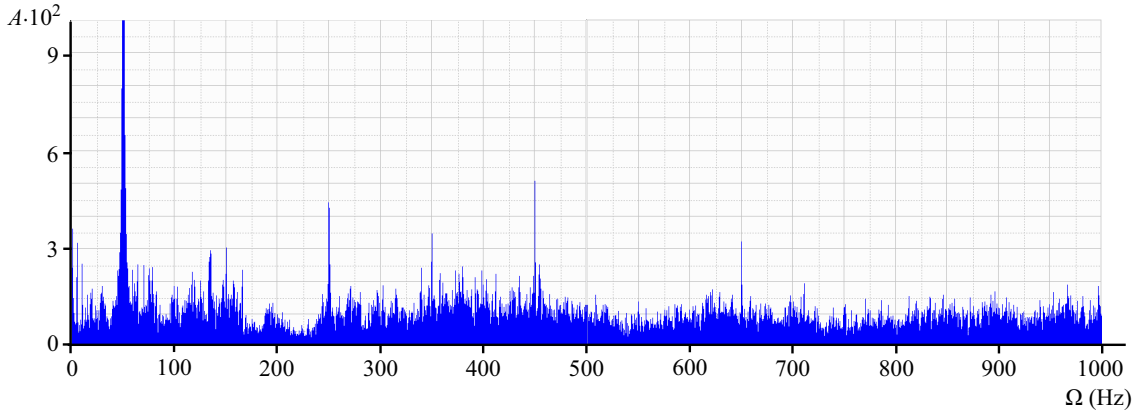

Figure 10: Typical spectrum of the wind tunnel wall vibration. All peaks with frequencies proportional to 50 and 100 Hz are electrical interferences and should be ignored.

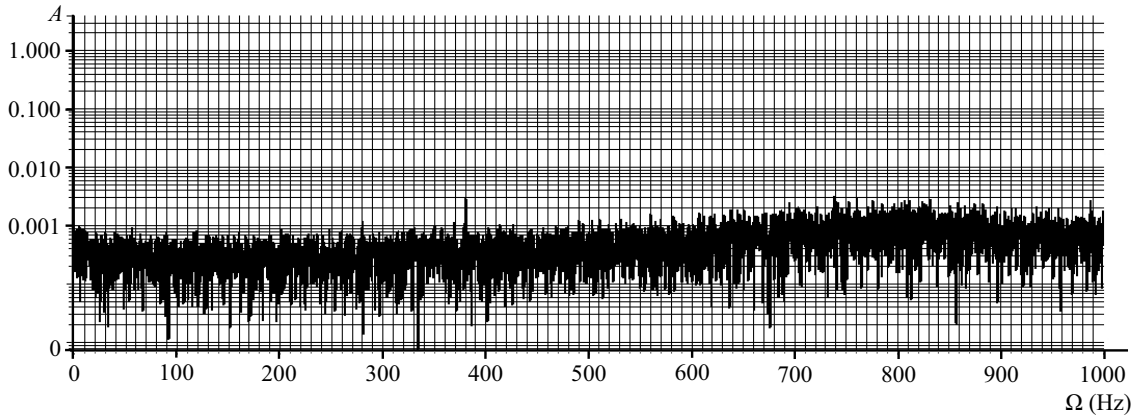

Figure 11: Typical spectrum of air pressure pulsation.

(1,1). Another peak, with frequencies 260 Hz at $M = 1.147$, 230 Hz at $M = 1.167$, 200 Hz at $M = 1.286$, and 215 Hz at $M = 1.298$, corresponds to the mode (2,1). We see that these peaks move along spectrum with change of M due to plate temperature effects, but not approach to each other. That is why there is no couled-type flutter.

Thus, all items, except single mode flutter, are excluded from the list of possible sources of amplication of the plate oscillations listed in Section 2. We therefore conclude that we observe single mode flutter at the region $1.2 < M < 1.3$.

6 COMPARISON WITH THEORETICAL RESULTS

As was theoretically shown in Section 3, at single mode flutter the most unstable modes are (1,1) and (2,1). This is exactly what we see in test spectrums (Figure 12, 13, 14, and 9): peak lying in region $160 \ldots 190$ Hz corresponds to the mode (1,1), peak lying in region $200 \ldots 260$ Hz corresponds to the mode (2,1).

Experimental single mode flutter boundary $M_{\text{cr}} \approx 1.2$ is very close to the theoretical value $M_{\text{cr}} = \min\limits_{m,n} M_1(m,n) = 1.17$ (Table 1).

Unfortunately, modes of other peaks presented in the spectrums were not recognized. The reason is residual stresses in the plate left after welding: natural modes were distorted due to presence of those stresses. Among distorted modes we are not able to distinguish number of

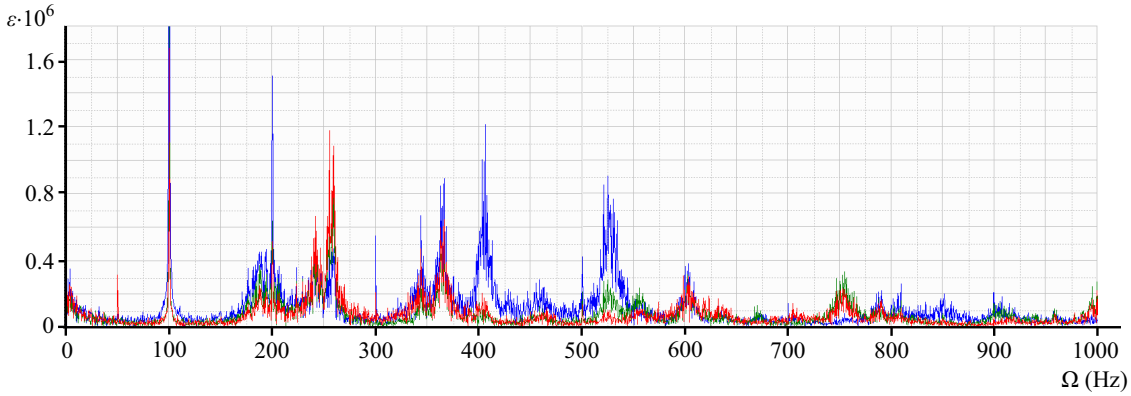

Figure 12: Spectrum of plate vibrations at regime $M = 1.147$. All peaks with frequencies proportional to 50 and 100 Hz are electrical interferences and should be ignored.

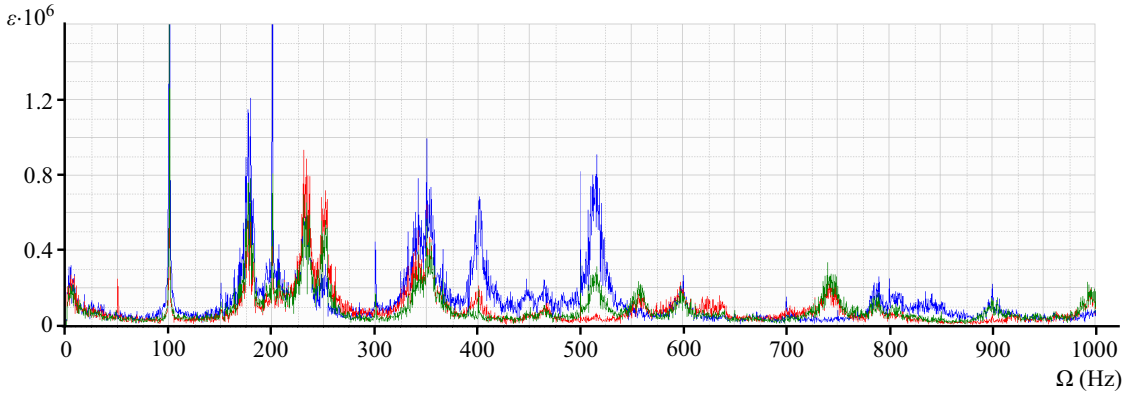

Figure 13: Spectrum of plate vibrations at regime $M = 1.167$. All peaks with frequencies proportional to 50 and 100 Hz are electrical interferences and should be ignored.

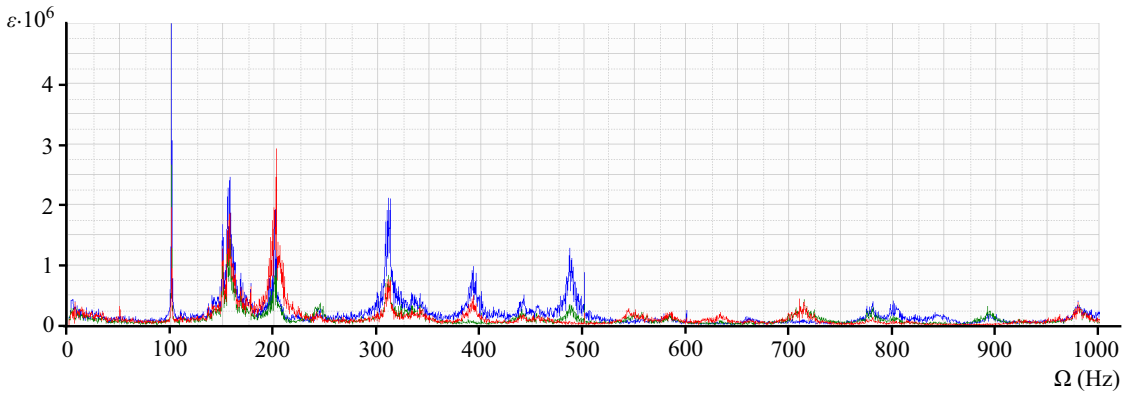

Figure 14: Spectrum of plate vibrations at regime $M = 1.286$. All peaks with frequencies proportional to 50 and 100 Hz are electrical interferences and should be ignored.

semi-waves in modes, because there are no more semi-waves. But we have theoretical results in Table 1, and we may assume that other peaks at flutter spectrums correspond to some of theoretically unstable modes (2,2), (3,1), (3,2), (4,1), (4,2).

There are two reasons why we are not worried about residual stresses distorting plate eigenmodes. First is the fact that the most flutter unstable modes (1,1) and (2,1) are not really affected

by those stresses, and physical mechanism of single mode flutter excitation [10] works. Another reason is that analysis and conclusions are made through test data only, not utilizing theoretical results. We investigated type of the plate vibration, in series excluding possible sources of vibrations from the list in Section 2, using only logical arguments based on the test data.

7 CONCLUSIONS

- A clamped steel plate is tested in a supersonic wind tunnel. The plate is intentionally chosen so that single mode flutter should occur, while "classical" coupled-type flutter is impossible.
- During the test, plate vibrations amplified in region $1.2 < M < 1.3$. Analysis of spectrums of the plate strain gages, pressure gage and wind tunnel vibro gage showed that the plate experienced single mode flutter.
- Test results excellently agreed with theory [10]: during the tests flutter occured at modes which are theoretically most unstable. Experimental flutter boundary $M_{\rm cr} \approx 1.2$ is very close to theoretical value $M_{\rm cr} = 1.17$.

The work is partially supported by Russian Foundation for Basic Research (08-01-00618) and by a Presidential Grant for the Support of Leading Scientific Schools (NSh-1959.2008.1).

REFERENCES

[1] V.V. Bolotin, *Nonconservative problems of the theory of elastic stability*. Pergamon Press, 1963.

[2] H.C. Nelson, H.J. Cunnigham, Theoretical investigation of flutter of two-dimensional flat panels with one surface exposed to supersonic potential flow. *NACA Report No. 1280*, 1956.

[3] Dun Min-de, On the stability of elastic plates in a supersonic stream. *Soviet Physics Doklady*, **3**, 479–482, 1958.

[4] Dowell E.H. Nonlinear oscillations of fluttering plate. II. *AIAA Journal*, **5 (10)**, 1856–1862, 1967.

[5] Dowell E.H. Generalized aerodynamic forces on a flexible plate undergoing transient motion in a shear flow with an application to panel flutter. *AIAA Journal*, **9 (5)**, 834–841, 1971.

[6] T.Y. Yang, Flutter of flat finite element panels in supersonic potential flow. *AIAA Journal*, **13 (11)**, 1502–1507, 1975.

[7] Dong Min-de, Eigenvalue problem for integro-differential equation of supersonic panel flutter. *Applied Mathematics and Mechanics*, **5 (1)**, 1029–1040, 1984.

[8] Dowell E.H., *Aeroelasticity of plates and shells*. Kluwer Academic Publishers, 1974.

[9] V.V. Vedeneev. Flutter of a wide strip plate in a supersonic gas flow. *Fluid Dynamics*, **5**, 805–817, 2005.

[10] V. V. Vedeneev. High-frequency flutter of a rectangular plate. *Fluid dynamics*, **4**, 641–648, 2006.

[11] V.V. Vedeneev. Nonlinear high-frequency flutter of a plate. *Fluid Dynamics*, **5**, 858–868, 2007.

[12] V.V. Vedeneev. Numerical investigation of supersonic plate flutter using the exact aerodynamic theory. *Fluid Dynamics*, **2**, 314–321, 2009.

[13] Movchan A.A. On stability of a panel moving in a gas. *PMM*, **21 (2)**, 231–243, 1957 (in russian).